Power Grid Vulnerability Analysis with Rising Renewables Infiltration

Saikat DAS, Zhifang WANG
Electrical and Computer Engineering Department, Virginia Commonwealth University
Richmond, Virginia 23220, USA

ABSTRACT[1]

The increasing penetration of renewable energy has a significant impact on the performance and reliability of the power grid. This is largely because of the uncertainty of the renewable resources and the complex nature of the power system infrastructure. This paper analyzed power grids' vulnerability to cascading failures with respect to the penetration level of renewable energy into the grid. In this paper, a novel power balance technique is used for cascading failure analysis and power grid vulnerability measurement. The proposed approach incorporates a modified optimal power flow algorithm in the grid vulnerability analysis study which accurately reflects the most probable path of cascading failure evolution process with uncertain renewable generation. The simulation results on IEEE 118 bus system, IEEE 300 bus system and 500 bus system showed that increasing penetration of renewable energy have proportionally higher impact on grid vulnerability to cascading failures due to injection of higher uncertainties into the grid. It was also evident that after a certain level of RE penetration, some system might deteriorate rapidly and preventive measures should be taken if and when RE penetration level exceeds that limit.

Keywords: Cascading Failure, AC Power Flow, Optimal Power Flow, Grid Vulnerability, Uncertainty.

1. INTRODUCTION

The modern power systems are undergoing some massive transitions. Growing demand of electricity, when combined with the need to limit carbon emissions to achieve sustainable development goals [1], encourages a rapid growth of renewables into the existing power system. However, the unpredictable nature of renewable sources will inject significant amount of uncertainty into the grid which may lead to cascading process resulting into blackout. So, it is necessary to study the impact of renewable energy (RE) penetration to grid vulnerability analysis to cascading failures (CF).

The literature on CF mainly focuses on the modelling and analytical tools for a given network. There are two types of models in simulating CF; transient models and steady state models. In [2], a dynamic model is presented which can simulate various cascading outage mechanisms. Steady state models are more common in literature to study and evaluate CF process. In [3], [4], the mixed OPF-stochastic models are the examples of steady state CF model where DC power flow (DCPF) was used to reduce computational burden. As DC models resulted in large errors in flow estimation [5] for large networks, [6], [7], are among the models incorporates AC power flow in the simulation of CF. In the stochastic CF model in [7], conventional optimal power flow (OPF) is used in the power balance algorithm which failed to accurately evaluate the negative impacts introduced by RE on the grid vulnerability.

In our proposed model, a new CF model with AC power flow (ACPF) method is used for vulnerability analysis of the grid network to cascading process. Cascading failure is a fast-evolving process. So rather than using conventional OPF, the proposed approach incorporates a modified OPF algorithm where least square adjustment method is used to restore the balance in the network during cascading failures and in result, the simulation process accurately mimics the most probable evolution path of CF process. To measure the vulnerability to CF, load shedding amount and number of tripped lines for increasing RE penetration are used as measuring tool in this study. Simulations have been performed on IEEE 118 bus system and IEEE 300 bus system for different testing cases and scenarios. This study has also revealed that after a certain level of RE penetration, system may deteriorate rapidly and preventive measures should be taken if and when RE penetration level exceeds that limit in order to mitigate the negative impacts of RE penetration during CF process.

The rest of the paper is arranged in following parts. In section 2, the system model is briefly discussed. Section 3 contains the modified OPF algorithm and the overall simulation workflow. Section 4 and 5 present results and conclusion, respectively.

2. SYSTEM MODEL

The modern power system is an ever-evolving complex infrastructure. Their complex interconnected nature along

[1] The authors wish to acknowledge and thank Dr. Hamidreza Sadeghian for his service in proofreading this manuscript.

with characteristics of different parameters introduce uncertainties into the network. Demand growth, availability of renewable energy sources, contingencies, climatic conditions, interconnections, power markets, are some examples of uncertain data. The goal of this study is to assess the grid vulnerability to cascading process from uncertainty perspective. Our proposed model considers uncertainty from load and renewable generation which propagates linearly in the line flow process.

A. Uncertainty modelling

In the proposed uncertainty model [8], the load demand power and renewable generator output power are represented with two terms as follows:

$$P(t) = \mu_p(t) + \epsilon_p(t) \tag{1}$$

where $\mu_P(t)$ is the mean of load demand power or renewable generator output power at time *t*. In other words, it is the expected power signal ahead of time. It is actually the forecasted power we achieve through some forecasting techniques using historical data. And $\epsilon_P(t)$ represents the uncertainty which is a zero-mean signal. It is the difference between forecasted data and actual data. In this study, we assume load forecasting errors and wind output power mismatches as uncertainties. As the historical data and future data follow same pattern for load demand and renewable resources, a widely popular forecasting model, Autoregressive Moving Average (ARMA) technique [9] is used to model uncertainties in this study.

B. Line flow based on AC power flow

The power flow study is the numerical computation of voltage magnitude and phase angle at each bus in an interconnected network under steady state condition. The DC power flow approximation is a common approach for calculating load flow and detecting overloaded branches. This approximation considers some assumption to achieve the linearization of power flow equations which results in reduction of computational burden. In DCPF, we assume flat voltage profile which means the voltage amplitude is equal for all nodes and voltage angle differences between neighboring nodes are small. We also assume line resistance are negligible compared to line reactance. The accuracy of DCPF depends on these assumptions' validity in real network situation. These assumptions do not hold true for AC power flow which may result in huge computational burden and convergence problem for large complex network. On the other hand, the accuracy of AC power flow solutions is much higher and we can access the voltage profile of the busses in the network. Due to these approximations DCPF underestimate the severity of cascading failure in large complex networks [5]. In our proposed cascading failure model, we have used ACPF to detect overloaded branches. However, to determine the mean flow in the branches Unscented Transformation (UT) method is used to avoid the disadvantages of ACPF [10], [11].

C. Unscented transformation

The unscented transformation (UT) method can overcome the limitations of linearization by providing a direct and definitive approach for transforming statistical information. UT method can provide higher accuracy with the same computational burden as linearization. The basic idea of UT method is that it is easier to estimate a probability distribution function than it is to estimate an arbitrary nonlinear function [12]. In UT method, the input points are selected in a way that they can maintain enough information to represent their probability distribution function.

The UT method is applicable to different uncertain problems with satisfactory result. This method calculates the statistics output random variables undergoing a set of nonlinear transformations. In our model, the inputs of the UT methods are the load demand and renewable generation. We have chosen the input points in a way so that we can determine the mean and covariance of the input variables. Then UT method can estimate the mean and covariance of the output random variables, in our case, line flow in the network [7]. Special focus should be given on the idea that, in the UT method, the sample points are not selected randomly. They are chosen in a specific way so that they have a predefined mean and covariance. This statistical information propagates through some nonlinear function and ultimately results in an accurate estimation of statistics of the output variable.

D. Tripping mechanism and relay model

In the proposed relay model, we have used the mean and covariance of the branch flow derived by the UT method. This statistical information is the main component of the CF simulation relay model. Here, power flow of each branch is assumed to be Gaussian to determine the normalized overload distance and in result, the overloading probability of each branch [3]. Then, we can calculate the mean overload time ($\overline{\tau_l}$) of branch *l* using the normalized overload distance (z_l) and overloading probability (ρ_l).

$$\overline{\tau_l} = \frac{2\pi\rho_l e^{\frac{z_l^2}{2}}}{BW_l} \tag{2}$$

Where, BW_l is the equivalent bandwidth of the flow process for the *l*th line [13].

This relay model introduces the uncertainties injected from RE sources and loads to the line flows. The time-inverse relay algorithm is in motion when the line becomes overloaded and the time to trip (t_{tr}) is inversely proportional to the line overloading value. This value is determined based on the thermal stability of the transmission lines [14]. This t_{tr} value is compared to the mean overload time, $\overline{\tau_l^u}$, if it is larger the trip timer is set to zero, otherwise, the trip timer is set to the relay time to trip. This tripping mechanism enables us to model the stochastic process of CF and identify the most probable path for its propagation.

3. MODIFIED OPF ALGORITHM

During cascading failure process, branches of the power grid may trip and become disconnected. The grid network changes after every line trip. To restore the balance in the system some modification may be required. In [7], author proposed a power balance algorithm to restore the balance. In this algorithm, conventional OPF is used which could not accurately evaluate the impacts of RE penetration into the grid during CF. As CF is a very fast evolving process, conventional OPF would not properly reflect the transition path of CF process after every line tripped. Here, we proposed a modified OPF algorithm which can restore the balance of the grid within its capacity limit. In this algorithm, we have proposed least square adjustment of the parameters of power grid within their valid capacity limit. The main goal of this algorithm is to mimic the most likely evaluation path of CF process in each step of the simulation process. The solution of this optimization problem restores the balance of the grid network within the least possible adjustment of generation and load controls in the grid and in result, accurately evaluates the impacts of RE penetration during CF process by representing the most likely transition path of CF process after every line trip.

A. Objective function

The objective function of this modified OPF is the least square adjustment of generation and load controls after every line tripping occurs. In this optimization problem, we try to minimize the differences of generation and load control parameters from their initial value. As oppose to the conventional OPF, it only focusses on real and reactive generation, real and reactive load demand and bus voltage magnitude. In CF process, every line tripping result in change of the existing network and the adjustment of generation and load is necessary. The modified OPF serve this purpose keeping the system as close to the initial condition.

$$\min_{P_G,P_D,Q_G,Q_D,V} \boldsymbol{W}[\ \|\Delta P_G\|_2^2\ \ \|\Delta P_D\|_2^2\ \ \|\Delta Q_G\|_2^2\ \ \|\Delta Q_D\|_2^2\ \ \|\Delta V\|_2^2\ ]^T \qquad (3)$$

Here, $\Delta P_G, \Delta Q_G, \Delta P_D, \Delta Q_D$ and ΔV represent the real power generation adjustment, reactive power generation adjustment, real load adjustment, reactive load adjustment and the voltage magnitude adjustment respectively for each bus before and after line tripping.
And, $\boldsymbol{W}$ represents coefficients or the penalty factors for the respective terms in optimization problem.
Here, $\boldsymbol{W} = [\ w_1\ w_2\ w_3\ w_4\ w_5]$. The values of these coefficients determine the gravity of their respective terms in the overall minimization problem. For example, in a specific case when minimizing load shedding is of top importance, one can put extra effort in minimize it by setting higher value of w_2 from other coefficients, which may result into other parameters shift away from initial value. In other cases, it could be of more importance to keep the differences of generation dispatch as less as possible. In that case, coefficient w_1 will be set to a higher value to minimize the difference of generation dispatch which may lead to higher amount of load shedding. Thus, the values of the coefficients can be chosen in a way to serve specific purpose in specific cases. Here, in our simulation, all the coefficient values are set to 1 to give equal importance to every term in the modified OPF algorithm.

B. Constraints

The modified OPF is a constrained optimization problem which has two types of constraints.

Equality Constraint: The active and reactive power balance in each bus, namely the AC power flow equation is the equality constraint set for this modified OPF.

$$f(V_m, \theta, S_{G,}\ S_D, Y) = 0 \qquad (4)$$

Here V_m represents bus voltage magnitudes, θ represents bus voltage angles, S_G is the complex generation power, S_D is the complex load and Y is the admittance matrix for the grid after line tripping occurs.

Inequality constraint: The operating limits of the components of power grid control the steady state operation of the network. These operating limits are the inequality constraints set for this modified OPF.

$$X_{min} \le X \le X_{max} \qquad (5)$$

Here X represents real and reactive generation, real and reactive load, bus voltage magnitude and bus voltage angle, X_{max} is the upper boundary and X_{min} is the lower boundary of the parameters. These are the inequality constrains of the modified OPF.

C. Algorithm

In CF simulation process, after every line tripping this modified OPF restores the balance of the network using least square adjustment of the generation and load controls Figure 1 shows the flowchart of the modified OPF. This modified OPF model represents a nonlinear constrained optimization problem. We have used an optimization toolbox of MATLAB, 'fmincon', to solve this problem. This modified OPF takes the transformed admittance matrix after tripping and power flow solution of the network before line tripping as inputs. The parameters are initialized as the power flow solution of the network before line tripping. The inequality constraints are set as the operating limits of the generation and load controls and the equality constraints are the real and reactive power balance equations for each bus.
In figure 3, the overall working diagram of proposed model has been shown. For a specific network we have chosen a few different scenarios where several generators were selected to replace them with wind generators. For every scenario, we have chosen different conventional generators for replacement. According to the load data, wind data and scenarios, we performed an initial optimal

power flow to determine the generation dispatch for different RE penetration. Then we introduced n-2 contingency into the system to initiate cascading failure.

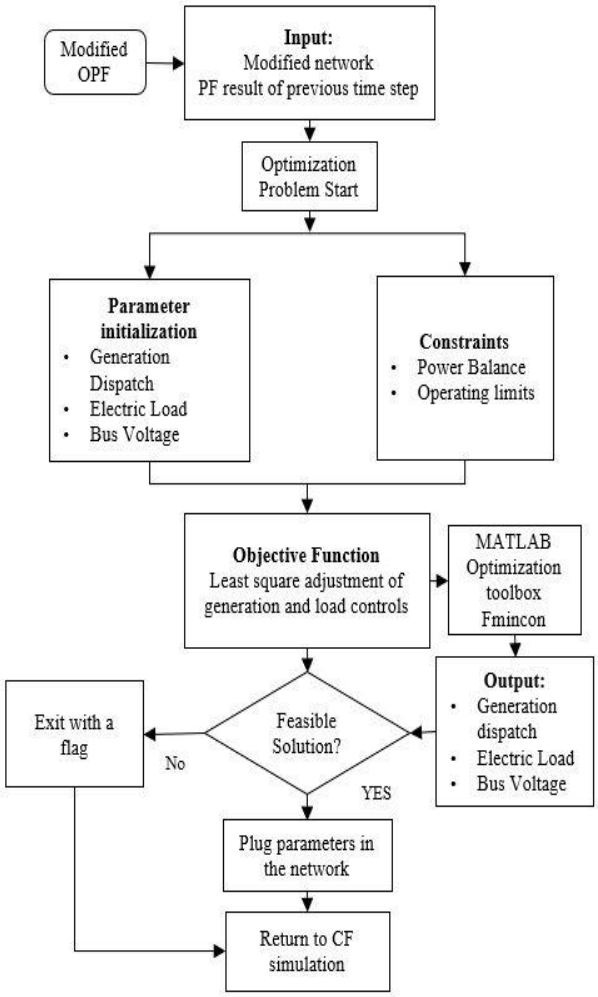

Fig 1. Flowchart of the modified OPF

After every line tripping, the modified OPF restored the power balance of the network with least square adjustments of the parameters within their boundary. In every time step, we performed power flow analysis to determine the overloaded lines. For every overloaded line, we have used UT method to find out mean overloading time and specific lines have been tripped when the trip timer hit zero. During cascading process, we have shut down all isolated buses and islands without generation. After the simulation, load shedding amount and number of tripped lines have been stored. For every scenario, we have used several different n-2 contingencies to initiate cascading process and took the average of load shedding and trip count to measure the severity of the cascading process. For every scenario, we have repeated the process for different level of RE penetration to see the impact of RE penetration level on the severity of cascading process.

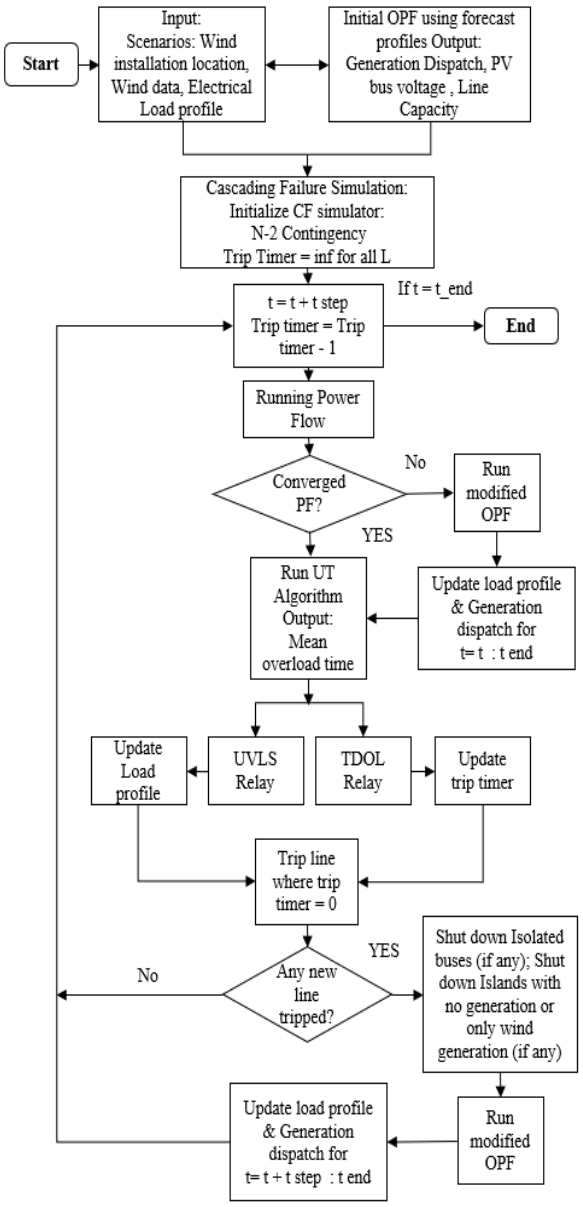

Fig 2. Overall overview of CF simulation

4. SIMULATION RESULTS AND DISCUSSION

We have simulated the impacts of increasing renewable generation integration on grid vulnerability to cascading overload failures in two IEEE standard cases (IEEE 118 and IEEE 300 bus system) and one synthetic 500 bus system (ACTIVSg500). In all the cases, we have selected a few different scenarios and several different initial n-2 contingencies to initiate cascading process. We have used four hours of load data and wind generation data with 4 second resolution.

Scenarios: In a specific scenario, we have selected six different conventional generators to replace those with wind generators. The six conventional generators have been selected in a way so that they could contribute at least

30% of the total generation of the system which in result, represents up to 30% RE penetration in the system. Then these conventional generators are gradually replaced by wind generators to see the effect of increasing RE penetration in the grid. In our simulation, we have chosen a limited number of scenarios in order to reduce the computational burden. The scenarios have been chosen in a way so that most of the conventional generators by turn could have been replaced by wind generators.

Contingency: To initiate the CF simulation, we have manually tripped two branches (n-2 contingency) at the initial stage of the simulation. We have selected several different n-2 contingencies to initiate the CF simulation to see different cascading failure evaluation path for every scenario. In order to reduce the computational work load, we have selected limited number of initial n-2 contingencies. The contingencies have been selected from a batch of contingencies which mostly represents the critical lines of the system which leads to CF process.

IEEE 118 Bus System: The IEEE 118 bus test case represents a portion of the American Electric Power with 54 committed generators, 99 loads and 186 branches [15]. The maximum generation capacity is 9966 MW and total average load is 4330 MW. We have considered fifteen different scenarios where we replaced conventional energy with wind energy to see the impact of RE penetration in case of cascading failure.

To initiate cascading failure, we introduced 50 different N-2 contingencies in the simulation for every scenario to see its evolution process. To measure the severity of the cascading process we considered the load shedding amount and trip count for every cases. For every scenario, we have tested our model for 0% to 30% renewable penetration. We have taken the mean of the total load shedding amount for 50 different initial n-2 contingencies. In scenario 1, generator 5, 10, 17, 21, 30 and 40 have been replaced by wind generator. We have simulated this scenario for 50 different n-2 contingencies. The average load shedding amount and average count of line tripping are the measuring tool to asses vulnerability to cascading failures.

TABLE I
VULNERABILITY IMPACTS EVALUATION (SCN 1)-IEEE118

Avg Load Shedding (MW)				Avg number of lines tripped			
RE 0%	RE 10%	RE 20%	RE 30%	RE 0%	RE 10%	RE 20%	RE 30%
22.19	63.49	131.95	175.84	2.54	4.02	4.98	5.90

From Table I, we can see that for scenario 1, with increasing renewable penetration, the average load shedding amount increased from 22.19 MW to 175.84 MW. And the average trip count also increased from 2.54 to 5.90. The increasing renewable penetration increased uncertainty into the system which results in larger amount of load shedding which makes the network more vulnerable to cascading failure.

From figure 3, we can see the same trend for every scenario, which is the increasing trend of load shedding amount with increasing RE penetration. If we take a closer look on figure 2, we can see that for 50% of cases there is a sudden increase in load shedding when RE penetration level reached 20%.

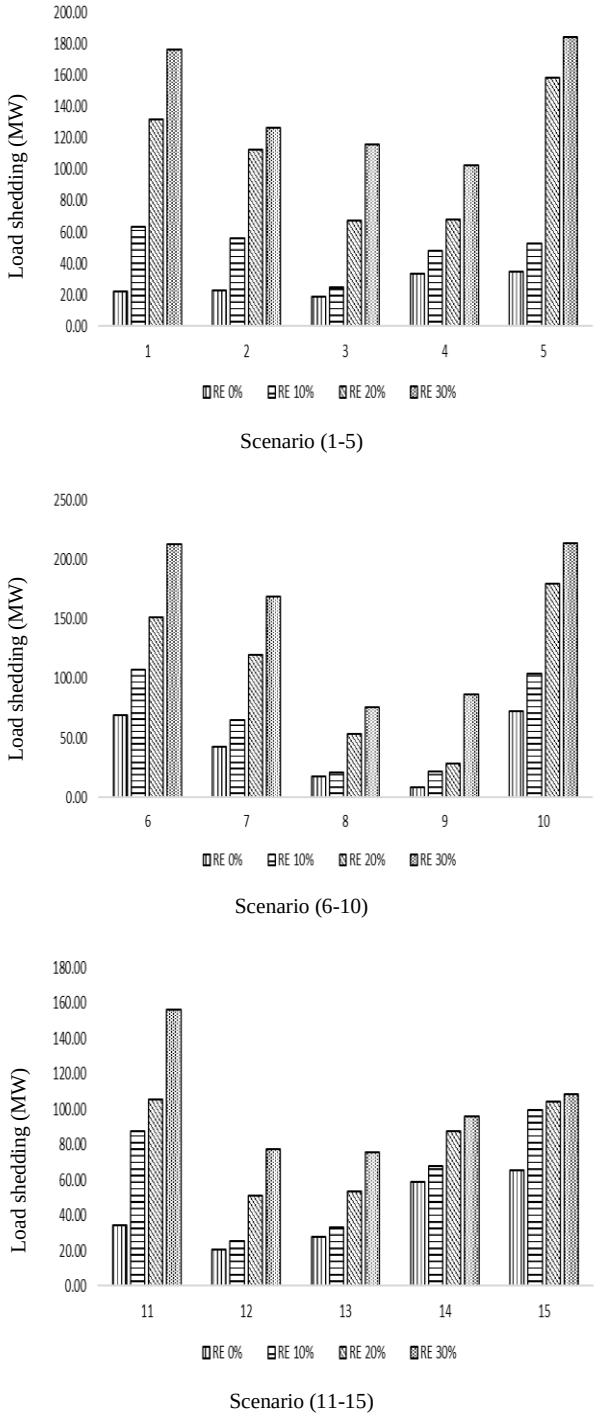

Fig. 3 Average load shedding amount for increasing RE penetration (IEEE 118 bus system)

In figure 4, we have shown the average number of line trips for every scenario with 50 different n-2

contingencies. The line trip count also increased with the increasing RE penetration.

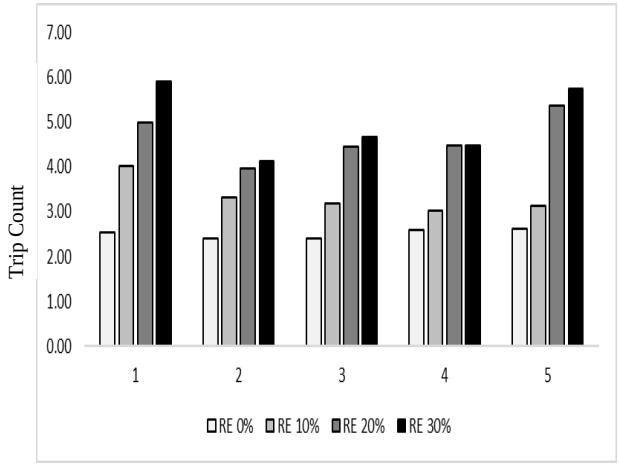

Scenario (1-5)

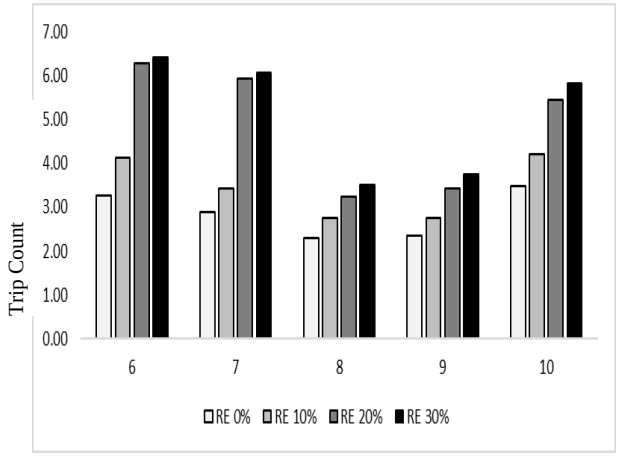

Scenario (6-10)

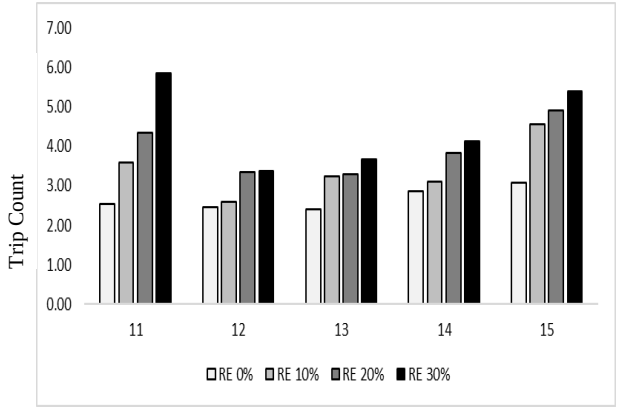

Scenario (11-15)

Fig. 4 Number of tripped lines for increasing RE penetration (IEEE 118 bus system)

For a specific scenario and for a specific contingency we can see the most probable cascading process evaluation path. In Table II, we can see that for scenario 1, when we initially tripped line 51 and 168 to initiate CF process, the trip count and the load shedding percentage increased with increasing RE penetration.

TABLE II
VULNERABILITY IMPACTS FOR A SPECIFIC CONTINGENCY-118 BUS

Scenario	N-2 Contingency	RE Penetration	Trip Count	LNS (%)
1	51, 168	0%	4	0.60
		10%	13	8.77
		20%	17	12.71
		30%	26	24.10

In figure 5, we can see the cascading failure evolution process for scenario 1 where branch 51 and 168 was initially tripped. We can see the initial escalation in the initial stage of the CF process and then after some time the system becomes stable. For RE penetration of 0% the system has stabilized very quickly compared to higher RE penetration level. With increasing RE penetration, the system took more time to stabilize which also indicates the vulnerability to CF with uncertain generation.

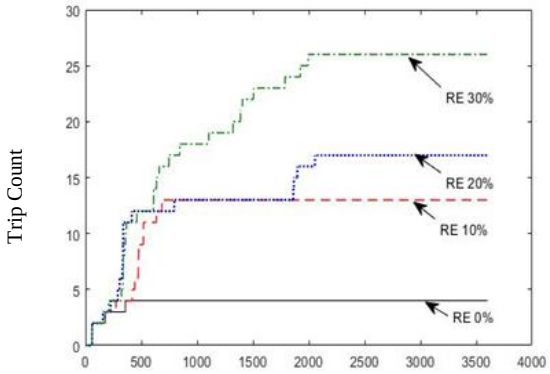

Time Step (4 second per step)

Fig. 5 Cascading failure evolution for a specific contingency

IEEE 300 Bus System: We have tested our algorithm on another IEEE test case, IEEE 300 bus system. This test case was developed by the IEEE test systems task force under the direction of Mike Adibi in 1993. This system contains 69 generators, 304 transmission lines and 195 loads, and its loading level is higher than 118 bus system [16]. The maximum generation capacity is 32,678 MW and the total load is 23,525 MW. We have considered ten different scenarios for this test case where we replaced conventional energy with wind energy to see the impact in case of cascading failure. To initiate cascading failure, we introduced N-2 contingencies in the simulation. For every scenario, we have considered 10 different n-2 contingencies to initiate cascading failure and see its most probable evolution process. To measure the severity of the cascading process we have considered the load shedding amount and trip count for every case as measuring tool.
For example, in scenario 2, generator 11, 14, 31, 48, 62 and 64 have been replaced by wind generator. We have simulated this scenario for 10 different n-2 contingencies.

The average load shedding amount and average number of tripped lines are the measuring tool to asses vulnerability to cascading failures.

TABLE III
VULNERABILITY IMPACTS EVALUATION (SCN 2)-300 BUS

Avg Load Shedding (MW)				Avg number of lines tripped			
RE 0%	RE 10%	RE 20%	RE 30%	RE 0%	RE 10%	RE 20%	RE 30%
346.4	420.1	613.2	1181.9	4	4.67	6.22	8.11

From Table III, we can see that for scenario 2, with increasing renewable penetration, the average load shedding amount increased from 346.4 MW to 1181.9 MW. And the average trip count also increased from 4 to 8.11.

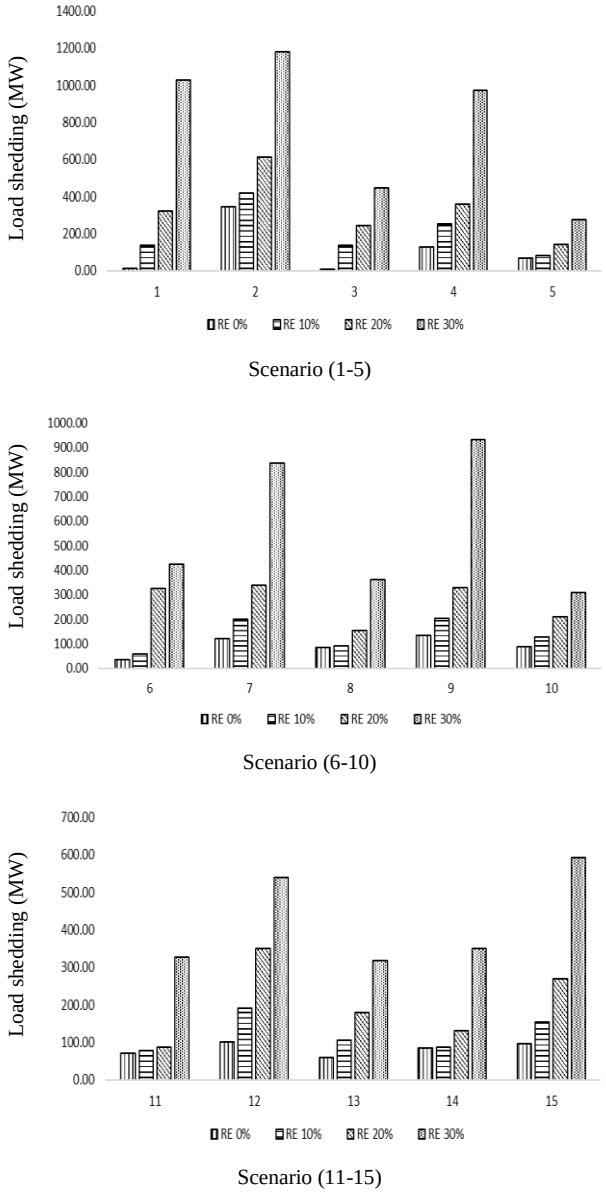

Fig. 6 Average load shedding amount for increasing RE penetration (IEEE 300 bus system)

The increasing renewable penetration increased uncertainty into the system which resulted into larger amount of load shedding and made the network more vulnerable to cascading failure.

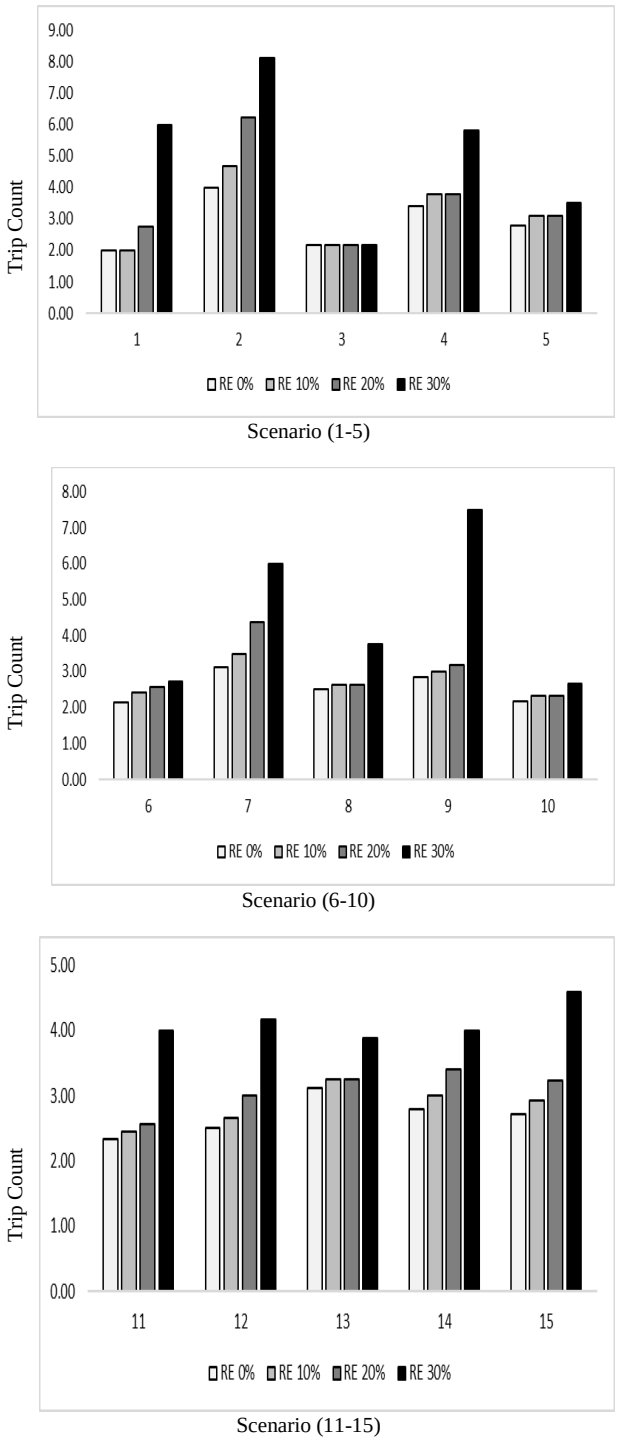

Fig. 7 Number of tripped lines for increasing RE penetration (IEEE 300 bus system)

From figure. 6 we can see the same trend for every scenario, which is the increasing trend of load shedding

amount with increasing RE penetration. If we take a closer look on figure 6, we can see that for almost 80% of the cases, when RE penetration level reached 30%, there is a rapid increase in load shedding amount which indicates that the system becomes more vulnerable at this level of RE penetration.
In figure 7, we have shown the average number of line trips for every scenario with 10 different n-2 contingencies. The line trip count also increased with the increasing RE penetration.

500 bus case (ACTIVSg500): The ACTIVSg500 case is a 500bus power system test case that is entirely synthetic, built from public information and a statistical analysis of real power systems. It bears no relation to the actual grid in this location, except that generation and load profiles are similar [17]. This system contains 56 committed generators, 597 transmission lines and 200 loads, total generation capacity 12188.9 MW and load 7750.7 MW. We have considered only three different scenarios for this test case due to high computational burden. To initiate cascading failure, we introduced N-2 contingencies in the simulation. For every scenario, we have considered 25 different n-2 contingencies to initiate cascading failure and see its most probable evolution process.

TABLE IV
VULNERABILITY IMPACTS EVALUATION (SCN 1)-500 BUS

Avg Load Shedding (MW)				Avg number of lines tripped			
RE 0%	RE 10%	RE 20%	RE 30%	RE 0%	RE 10%	RE 20%	RE 30%
230.2	268.6	280.6	303.9	6.05	6.53	6.68	6.79

From Table IV, we can see that for scenario 1, with increasing renewable penetration, the average load shedding amount increased from 230.2 MW to 303.9 MW. And the average trip count also increased from 6.05 to 6.79.

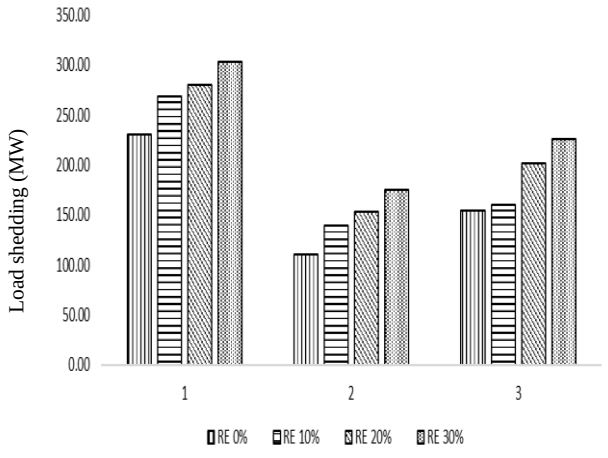

Fig. 8 Average load shedding amount for increasing RE penetration (500 bus system)

From figure. 8 we can see the same trend for every scenario, which is the increasing trend of load shedding amount with increasing RE penetration. If we take a closer look on figure 8, we can see that there is a steady increase in load shedding amount.
In figure 9, we have shown the average number of line trips for every scenario with 25 different n-2 contingencies. The line trip count also increased with the increasing RE penetration.

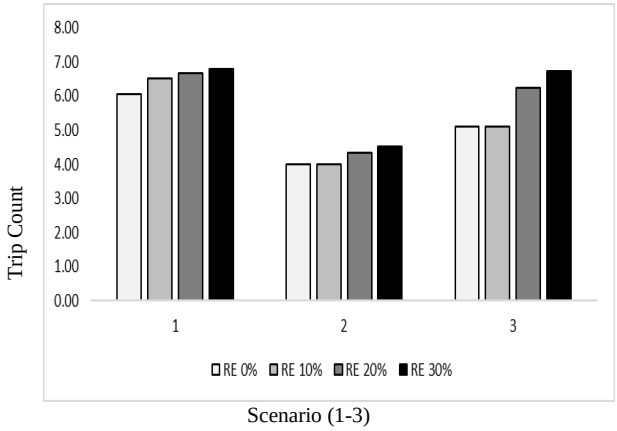

Fig. 9 Number of tripped lines for increasing RE penetration (500 bus system)

Comparing the results of the three cases we can say that, in all the cases with increasing penetration of RE, the amount of load shedding and the number of tripped lines increased. As measuring tool of vulnerability to cascading failure, the system becomes more vulnerable to cascading failure. Moreover, from figure 6, we can notice sudden rapid increase of load shedding amount for most of the scenarios in 300 bus system when RE penetration increases from 20% to 30%. As a matter of fact, on an average there is around 120% increase of load shedding when RE penetration increased from 20% to 30%.

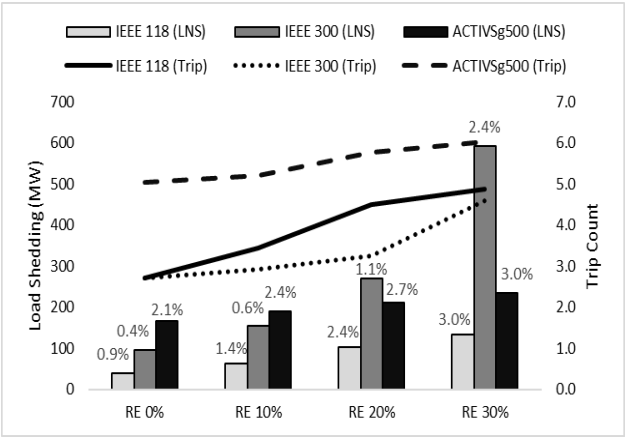

Fig. 10 Overall vulnerability analysis

From figure 10, we can see the overall vulnerability analysis for IEEE 118 bus system, IEEE 300 bus system

and 500 bus system averaging all the scenarios. The IEEE 118 bus system has the lowest loading level (43%) out of these three cases. We can see that for IEEE 118 bus system, load shedding reached 2.35% (102 MW) for 20% RE penetration. For IEEE 300 bus system, the loading level is the highest (72%). There is a sudden increase in load shedding (2.4%) when RE penetration reached 30%. As the total load amount (23,525 MW) is larger than the other two cases for IEEE 300 bus system, the load shedding amount (270 MW) is higher in that case. And for synthetic 500 bus system, the loading level (64%) is in between the previous two cases. We can see a steady increase of load shedding amount with increasing RE penetration which starts from 2.1% (165MW) load shedding for 0% RE penetration and ends up with 3% (235MW) load shedding for 30% RE penetration. The reason behind the high load shedding amount in 0% RE penetration is the selection of scenarios. For 500 case system, the three scenarios are chosen in a way to result in severe cascading failure process. Among the three cases, IEEE 300 bus system is more sensitive to RE penetration and infrastructure upgradation is necessary for this case.

It is evident that, for some cases when RE penetration reached a certain point, the system may enter a critical stage where it can deteriorate rapidly and preventive measures should be taken to mitigate the negative impacts of RE penetration. Hence, by incorporating the modified OPF power balance algorithm in simulation process, the negative impacts introduced by RE on the grid vulnerability have been accurately reflected.

5. CONCLUSIONS

In this paper, we have analyzed the impacts of renewable generation on grid vulnerability to cascading overload failures in terms of its penetration level. A full ACPF model with UT method and modified OPF for power balance have been used in the simulation process to accurately mimic the most likely evolution path of CF process and to make the study more accurate. Blackout size and number of tripped lines have been used as measuring tools to asses vulnerability to CF. It is found that higher penetration from renewable energy leads to higher number of trip count and larger amount of load shedding. The proposed model has also been able to identify that after a certain level of RE penetration, some system may deteriorate rapidly and preventive measures should be taken if and when RE penetration level exceeds that limit. As a future extension of this study, it is of interest to incorporate mitigation tools to prevent or minimize the severity of cascading failure in case of higher penetration of renewables.

6. ACKNOWLEDGMENT

The authors wish to thank Dr. Hamidreza Sadeghian for his insightful comments, suggestions, and critiques.

7. REFERENCES.

[1] "Social Development for Sustainable Development | DISD." https://www.un.org/development/desa/dspd/2030agenda-sdgs.html (accessed Nov. 05, 2020).

[2] J. Song, E. Cotilla-Sanchez, G. Ghanavati, and P. D. H. Hines, "Dynamic modeling of cascading failure in power systems," *IEEE Trans. Power Syst.*, vol. 31, no. 3, pp. 2085–2095, 2016, doi: 10.1109/TPWRS.2015.2439237.

[3] M. H. Athari and Z. Wang, "Impacts of wind power uncertainty on grid vulnerability to cascading overload failures," *IEEE Trans. Sustain. Energy*, vol. 9, no. 1, pp. 128–137, 2018, doi: 10.1109/TSTE.2017.2718518.

[4] M. H. Athari and Z. Wang, "Studying cascading overload failures under high penetration of wind generation," in *IEEE Power and Energy Society General Meeting*, Jan. 2018, vol. 2018-January, pp. 1–5, doi: 10.1109/PESGM.2017.8274358.

[5] H. Cetinay, S. Soltan, F. A. Kuipers, G. Zussman, and P. Van Mieghem, "Analyzing cascading failures in power grids under the AC and DC power flow models," *Perform. Eval. Rev.*, vol. 45, no. 3, pp. 198–203, 2018, doi: 10.1145/3199524.3199559.

[6] W. Ju, K. Sun, and R. Yao, "Simulation of cascading outages using a power-flow model considering frequency," *IEEE Access*, vol. 6, pp. 37784–37795, 2018, doi: 10.1109/ACCESS.2018.2851022.

[7] M. H. Athari and Z. Wang, "Stochastic cascading failure model with uncertain generation using unscented transform," *IEEE Trans. Sustain. Energy*, vol. 11, no. 2, pp. 1067–1077, 2020, doi: 10.1109/TSTE.2019.2917842.

[8] M. H. Athari and Z. Wang, "Modeling the uncertainties in renewable generation and smart grid loads for the study of the grid vulnerability," in *2016 IEEE Power and Energy Society Innovative Smart Grid Technologies Conference, ISGT 2016*, Dec. 2016, doi: 10.1109/ISGT.2016.7781265.

[9] S. J. Huang and K. R. Shih, "Short-term load forecasting via ARMA model identification including non-Gaussian process considerations," *IEEE Trans. Power Syst.*, vol. 18, no. 2, pp. 673–679, May 2003, doi: 10.1109/TPWRS.2003.811010.

[10] S. J. Julier and J. K. Uhlmann, "Unscented filtering and nonlinear estimation," in *Proceedings of the IEEE*, Mar. 2004, vol. 92, no. 3, pp. 401–422, doi: 10.1109/JPROC.2003.823141.

[11] M. Aien, M. Fotuhi-Firuzabad, and F. Aminifar,

"Probabilistic load flow in correlated uncertain environment using unscented transformation," *IEEE Trans. Power Syst.*, vol. 27, no. 4, pp. 2233–2241, 2012, doi: 10.1109/TPWRS.2012.2191804.

[12] S. J. Julier and J. K. Uhlmann, "Unscented Filtering and Nonlinear Estimation," 2004, doi: 10.1109/JPROC.2003.823141.

[13] Z. Wang, A. Scaglione, and R. J. Thomas, "A Markov-transition model for cascading failures in power grids," in *Proceedings of the Annual Hawaii International Conference on System Sciences*, 2012, pp. 2115–2124, doi: 10.1109/HICSS.2012.63.

[14] "ISBN 9780979142703 - Overhead Conductor Manual 2nd Edition Direct Textbook." https://www.directtextbook.com/isbn/9780979142703 (accessed Nov. 22, 2020).

[15] "Description of case118." https://matpower.org/docs/ref/matpower5.0/case118.html#_top (accessed Nov. 21, 2020).

[16] "IEEE 300-Bus System." https://electricgrids.engr.tamu.edu/electric-grid-test-cases/ieee-300-bus-system/ (accessed Dec. 29, 2020).

[17] "SouthCarolina 500-Bus System: ACTIVSg500." https://electricgrids.engr.tamu.edu/electric-grid-test-cases/activsg500/ (accessed May 11, 2021).